Available online at www.sciencedirect.com
SCIENCE DIRECT
Journal of Chromatography A, 1099 (2005) 103–110
JOURNAL OF CHROMATOGRAPHY A
www.elsevier.com/locate/chroma

Effect-directed analysis by high-performance liquid chromatography with gas-segmented enzyme inhibition

Susanne Fabel, Reinhard Niessner, Michael G. Weller *

Institute of Hydrochemistry, Technische Universität München, Marchioninistrasse 17, D-81377 München, Germany

Received 13 May 2005; received in revised form 12 August 2005; accepted 29 August 2005
Available online 28 September 2005

Abstract

A reversed-phase high-performance liquid chromatography system with UV-detector was equipped with an on-line acetylcholinesterase inhibition assay to achieve effect-directed analysis of potentially toxic samples. The enzyme activity was detected colorimetrically using Ellman's reagent. The inhibition and substrate conversion took place in glass capillaries at a 100 μL/min flow rate. Extra-column band spreading in the reaction coils reduces the sensitivity and separation power of biochemical detectors severely. Knitted reactors exhibited no reduction of longitudinal dispersion in the tested flow range. The implementation of air-segmentation allowed an extended inhibition and substrate conversion time without a significant loss of chromatographic resolution. The limit of detection of two model compounds carbofuran (carbamate) and paraoxon-ethyl (organophosphate) was determined to be 13 ng (injected mass) and 7.4 ng, respectively, applying an isocratic chromatography method. A mixture of five insecticides was separated by a gradient elution and the inhibitory effect on the enzyme activity could be detected with high resolution. The band width at half height of the enzyme inhibition detector signal after a reaction time of about 8 min or 4.2 m of capillary, respectively, increased only by a factor of 1.4 compared to the UV-detector signal.

Keywords: Bioresponse-linked instrumental analysis; High resolution screening; Biosensor; Air-segmentation; Segmented flow; Knitted reactor; Band broadening; μ-TAS; AChE

1. Introduction

Ground and surface water may be contaminated by an enormous variety of compounds. Public health authorities need to monitor the quality of water-bodies for drinking water supply and leisure time activities. One approach for the risk assessment is based on chemical analysis. The toxicity may be then modelled by individual toxicity parameters [1]. This procedure has two disadvantages. First, if main contaminants or metabolites are unknown, the model may fail completely. Second, the total chemical analysis is time-consuming, cost intensive and a flood of mainly irrelevant data is produced. Another approach for the toxicological risk assessment is based on biotests with various organisms (for an overview see [2]). Compounds affecting the test system can be detected without further knowledge about their identity. However, despite the specific relevance to the test organisms, the biotesting approach gives rarely any information about the identity of toxic compounds and only toxicological sum parameters are obtained.

A promising tool for the identification of compounds with toxic potential is the effect-directed analysis [3]. A suspect water sample is chemically analyzed, e.g. by HPLC and a toxic potential is assessed combining the separation step with a biomolecular recognition step [4–6]. For the hyphenation of chemical separation and toxicological assessment, several methods exist, similar to immunochromatographic techniques [7]. Instead of antibodies, reagents with toxicological relevance (such as enzymes or receptors) are used to identify the compounds. Simple biochemical tests can not simulate the complexity of the human metabolism, however, compounds recognized by these molecular targets can indicate potential hazards. Depending on the different strategies of effect-directed analysis, the biomolecular recognition step is used before or after the separation, either in an off-line or more sophisticated in an online mode. In the pre-column approach the compounds are affinity-enriched prior to

* Corresponding author. Tel.: +49 89 2180 78241; fax: +49 89 2180 78255.
E-mail address: michael.weller@ch.tum.de (M.G. Weller).
URL: http://www.ch.tum.de/wasser/weller/.

0021-9673/$ – see front matter © 2005 Elsevier B.V. All rights reserved.
doi:10.1016/j.chroma.2005.08.081

chemical analysis on immobilized recognition molecules analogous to immunoaffinity extraction procedures. For the detection of estrogenic compounds the combination of estrogen receptor assay and HPLC was proposed [8]. Another strategy of effect-directed analysis is to use the biochemical test after the separation step. This has several advantages, as the chromatographic separation step usually leads to a sample clean-up. Matrix effects are reduced and the reproducibility of the biochemical assay is improved. Furthermore, cross-reactivities of sample compounds are easier to handle and make inhibition tests, which are sometimes unreliable [9], more dependable. One option for an off-line biochemical test, is to collect and investigate only the peaks detected by UV absorbance [2] or to fractionate the whole chromatogram into a microplate for further biotesting. Estrogen receptor assays [10] and protein phosphatase inhibition assays [11] were reconstructed relative to the retention time of the chromatographic run and so-called biograms or enzymograms were obtained. In the case of high-performance thin-layer chromatography, the biochemical tests can be performed directly on the plate [12]. Testing of the whole chromatogram has the advantage, that compounds which were not observable by the respective conventional detector are not overlooked. Technically more demanding but less time-consuming is the on-line biochemical detection after chromatography. For the continuous-flow biochemical detection various detection methods can be used [13]. One detection principle is the competition of analyte and added labelled ligands of the biomolecular target. The detection signal is based on the separation of free and bound ligands, which can be achieved by restricted-access materials [14], receptor affinity columns [15] and hollow-fibre modules [16]. Immobilized enzyme reactors (IMER) [17,18] work without the need of labelled ligands. In this module, only an enzyme substrate has to be added. The difficulty of the IMER is to retain the activity of the enzyme during the immobilization procedure and the analysis. The detection of the substrate conversion depending on the enzyme activity is the principle of the IMER, as well as of the homogenous biochemical detector. In the latter, the enzyme and substrate solutions are pumped continuously to the mobile phase. Appropriate dilution of the eluent is necessary in most cases to avoid deactivation of enzyme in absence of inhibitors. Homogenous enzyme inhibition assays were successfully combined with liquid chromatography using alkaline phosphatase [19], phosphodiesterase [20], angiotensin-converting enzyme [21] and acetylcholinesterase [22,23]. For a further investigation of the substances which were targeted by enzyme inhibition, mass spectrometry parallel to the biochemical detector was proposed [19,21,22]. Recently, electrospray ionization MS was applied to simultaneously detect both the inhibitors and the enzyme activity without further need of an optical detector [24].

The reaction time in the biochemical assay is determined by the enzyme inhibition and the substrate conversion kinetics. The necessary residence time is attained by a reaction coil and an appropriate flow rate. Microfluidic components combined with a low flow rate may be used for low reagent consumption [25]. With these boundary conditions, the stream is strictly laminar. Not only the proper mixing of eluent and reagent becomes a problem. In addition, the parabolic flow profile leads to a severe longitudinal dispersion of the mobile phase. Band spreading is one of the main obstacles for effect-directed analysis using an enzyme inhibition assay. This problem also limits the gain in signal intensity by extended reaction times. Dispersion leads to a loss in signal intensity and the high resolution of HPLC can not be retained in the enzymogram. Therefore, the enzyme inhibition detection coupled to LC is restricted to short reaction times in short coils. This severely limits the choice of useful enzymes and the sensitivity of inhibitor detection.

The problem of extra-column band spreading in post-column reactors is well investigated [26–28]. Different methods were reported to overcome this problem. Packed bed reactors and coiled or knitted tube reactors [29,28] have been recommended. Coiling the tubing should induce a secondary flow perpendicular to the parabolic laminar flow profile. Then a radial mass transfer from the tubing axis to the wall is induced by centrifugal forces acting on the liquid stream. As a result, the parabolic flow profile is disturbed by the fluid circulating above and below the tubing axis and the dispersion along the longitudinal axis is reduced. The knitted tube reactors have been applied especially for post-column derivatization reactors, which worked in the milliliter per minute flow range with short reaction times [30,31]. However, the influence of the tube geometries for the reduction of band spreading seems to play only a minor role for microfluidic applications [32], which we could confirm by a model experiment.

Another method to reduce the band broadening is the segmentation of the stream into small reaction volumes. The technique of segmented stream reactors as post-column detectors is well known for slow reactions [27]. Usually, gas bubbles or droplets of a nonmiscible liquid are introduced into the effluent at regular time intervals. The higher the segmentation frequency, the smaller is the band broadening [33,34]. A colorimetric FIA system with air-segmentation for a reduction of longitudinal dispersion known as “AutoAnalyzer” was introduced first by Skeggs [35,36] in 1957. Later, the coupling of HPLC with an air-segmented post-column reactor was used for derivatization reactions [37,38]. Also chromatography combined with enzyme inhibition assays using acetylcholinesterase was reported many years ago [39–41]. Recently, the segmented flow methods are enjoying a renaissance [42–46]. Particularly, in micro total analysis systems (μ-TAS) the problem of rapid mixing without excessive dispersion has to be solved [47–49]. The advantages of miniaturization in FIA was shown for a gas-segmented continuous-flow analysis system, in which microbore tubing was used [50].

Here, we want to present the effect-directed analysis of toxic compounds based on high-performance liquid chromatography with enzyme inhibition detection, including an gas-segmented flow system, which works in the range of a 100 μL/min flow rate. As a model for a neurotoxic effect, an acetylcholinesterase engineered for biosensor applications was used [51]. Gas-segmentation in silica capillaries was used for enzyme inhibition and substrate reaction to overcome the problem of extreme band broadening in a homogenous enzyme inhibition system.

2. Experimental

2.1. Abbreviations

AChE, acetylcholinesterase; ATCI, acetylthiocholine iodide; DTNB, 5,5′-dithiobis-[2-nitrobenzoic acid]; EID, enzyme inhibition detection; HPLC–EID, HPLC with on-line EID; HPLC–SFEID, HPLC with on-line segmented flow EID; LOD, limit of detection; MTP, microtiter plate; NBS, *N*-bromosuccinimide; PBS, phosphate-buffered saline.

2.2. Reagents and chemicals

AChE of the nematode *Nippostrongylus brasiliensis* (enzyme mutant [51] produced in the yeast *Pichia pastoris*) was kindly supplied by H. Schulze and T.T. Bachmann (ITB, Stuttgart, Germany). DTNB, NBS, as well as all chemicals for the preparation of buffers were obtained in the highest purity available from Sigma (Taufkirchen, Germany). ATCI, gelatine from porcine skin (Bio-Chemika) and acetic acid (analytical-reagent grade for HPLC) were purchased from Fluka (Neu-Ulm, Germany). The pesticide standards as well as methanol and acetonitrile (both Chromasolv for HPLC, gradient grade) were obtained from Riedel-de Haën (Seelze, Germany).

Tris–HCl (pH8.0, 100 mM) containing 0.1% gelatine was used as enzyme dilution buffer. The enzyme for the microplate assay had a concentration of 10 mU/mL whereas the concentration for the HPLC–SFEID was 20 mU/mL. One unit of AChE will hydrolyze 1 μmol of acetylthiocholine per min at pH 8.0 at 37 °C. DTNB was dissolved in PBS freshly prior each experiment to obtain a 25 mM solution. ATCI was dissolved freshly in Millipore water to obtain a 100 mM solution. For the microplate assay, one volume of the ATCI solution and five volumes of the DTNB solution were mixed with four volumes of water to obtain the substrate/reagent solution. For the HPLC–EID measurements one volume of the ATCI solution was mixed with one volume of the DTNB solution.

The pesticide standards were dissolved in methanol to obtain stock solutions (10 mM) and stored in the refrigerator. For the injection into the HPLC and measurements in the microplate assay, the solutions were diluted with water to obtain appropriate dilutions with not more than 10% of methanol. For the oxidation of the phosphorothionate chlorpyrifos-methyl, 1780 μL of water, 200 μL of pesticide solution (1 mM in methanol) and 20 μL NBS solution (0.4 g/L in water) were stirred at room temperature for 30 min. The reaction solution was injected directly without further purification.

2.3. Enzyme inhibition assay on a microtiter plate

The AChE activity was determined according to the method of Ellman et al. [52] with some modifications. For optimization of the on-line enzyme inhibition detection, first experiments were performed in flat-bottomed polystyrene plates from Greiner (96-well, Nürtingen, Germany). Every experiment was done in triplicates. The inhibitory effect of the mobile phases on the enzyme was tested. Organic solvent/water mixtures (180 μL) were incubated with enzyme solution (20 μL) for 5 min at 37 °C. Twenty microliters of ATCI/DTNB solution was added and the color development was measured for 30 min every 30 s with a microtiter plate reader.

The ratio of enzyme and sample solution was changed in the later experiments to reduce the negative influence of organic solvents on the enzyme. The inhibitory effect of the pesticides was tested then by the incubation of sample solution (20 μL) with enzyme solution (180 μL). The remaining enzyme activity was calculated as the ratio between slope of absorbance signal (ΔA) with inhibitor and without inhibitor (Eq. (1))

$$\text{Activity AChE\%} = \frac{\Delta A_{\text{Inhibitor}}}{\Delta A_{\text{Blank}}} \times 100 \quad (1)$$

2.4. Setup of the HPLC–SFEID system

The setup of the segmented flow (SF) system is shown in Fig. 1. The chromatography system consisted of an on-line degasser (model DG-1310, Gynkotek, Germany), a HPLC pump (**1**) (High Precision pump model 480, Gynkotek, Germany) and a manual sample injection valve (model 7125, Rheodyne, Bensheim, Germany) with a 20 μL sample loop. The column used for chromatography was a Luna C18(2), 5 μm, 5 cm × 2.0 mm from Phenomenex (Aschaffenburg, Germany). Water containing 0.1% acetic acid (A) and methanol (B) were used as mobile phases. The flow rate was set to 200 μL/min. In the case of isocratic chromatography, 50% A and 50% B were mixed. For the separation of more than two pesticides, a gradient separation was carried out. The column was equilibrated at 90% A and 10% B. From the starting time to minute 1 the concentration of A decreased steeply to 65%. Then a linear decrease to 30% A at minute 11 followed. With a third linear step the concentration of A reached 10% at minute 13. From minutes 13–15, the concentration of A was held at 10% A.

The eluate was split into two streams, one to the UV detector (model 4225, Unicam, Kassel, Germany) and the other to the enzyme inhibition detection unit. A customized make-up flow splitter (Sunchrom, Friedrichsdorf, Germany) was used for the splitting and the subsequent mixing of eluate with enzyme solution. With a fixed split ratio of 1:20, 10 μL/min of the eluate were mixed with 90 μL/min of enzyme solution. The flow of the enzyme solution was achieved with a 10-mL syringe installed in a pump (**2a**) from Harvard Apparatus (model PHD 2000, Holliston, MA, USA). The fluid passed a T-piece (P-712, Upchurch Scientific, Oak Harbor, WA, USA). In the case of gas-segmentation, the third port of the T-piece was open to the air.

The mobile phase with potential inhibitors and the AChE were pumped into a reaction coil made of a silica capillary with a length of 270 cm and an inner diameter of 530 μm (Polymicro Technologies, Phoenix, AZ, USA). Typical incubation times were 5.6 min without segmentation, whereas with gas-segmentation it was 5.1 min. After the incubation, the ATCI/DTNB mixture was added with pump (**2b**) (250 μL-syringe) with a flow rate of 2.25 μL/min. The color development took place in a silica capillary with a length of 150 cm and an inner diameter of 530 μm. A typical development time was

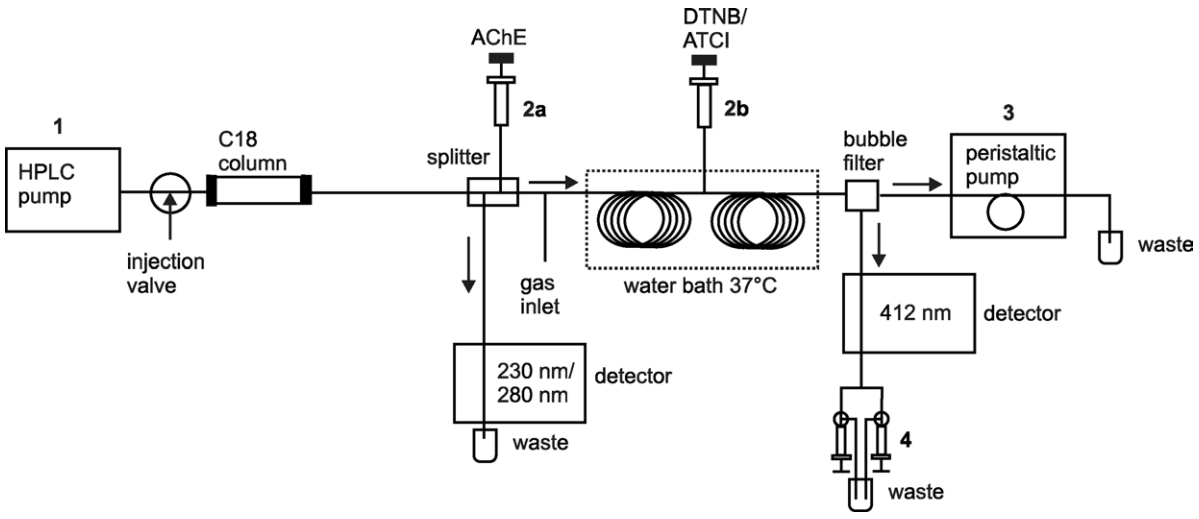

Fig. 1. Setup of the HPLC–SFEID (segmented flow enzyme inhibition detector). After the RP-HPLC system, the mobile phase was split. One part (190 μL/min) went to a conventional UV detector, the second part (10 μL/min) of the mobile phase to the SFEID. Enzyme solution and substrate/reagent solution were added continuously. The reaction took place in thermostated reaction coils. Air segments could be inserted by negative pressure generated by the peristaltic pump 3.

3.2 min without segmentation, whereas with gas-segmentation it took 2.7 min. The inhibition reaction coil as well as the color development coil were thermostated at 37 °C in a water bath.

The regular insertion of air bubbles into the system was achieved by negative pressure generated with a peristaltic pump **3** (Ismatec SA, Glattbrugg, Switzerland). By variation of the aspiration rate of the peristaltic pump, the intervals of the air bubbles can be influenced. The enzyme activity was recorded at 412 nm by an UV–Vis detector (model K2501, Knauer, Berlin, Germany) with a micro flow cell (path length 8 mm, inner diameter 150 μm, LC-Packings, Amsterdam, The Netherlands).

As expected, a short distance between the air segments severely disturbed the signal of the detector. Therefore, the bubbles had to be removed before the liquid flow entered the detector. A nearly complete removal was achieved by a bubble filter engineered in-house. The filter was manufactured of acrylic glass with two 250 μm bore holes at an angle of 90° and a third bore hole for inserting a membrane (Whatman grade 40, 8 μm pore size, cellulose, Brentford, Middlesex, UK) shown in Fig. 2.

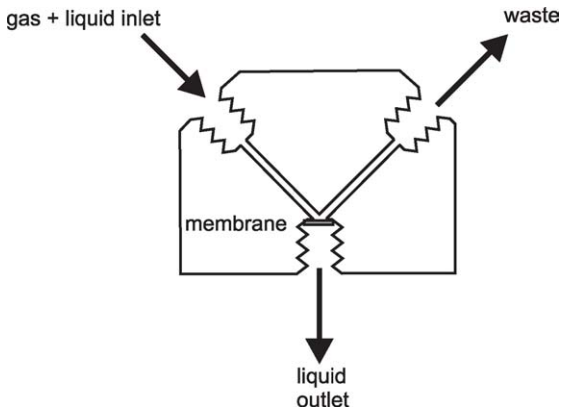

Fig. 2. Scheme of the bubble filter. For reliable detector signals, the air bubbles from the gas-segmented stream have to be removed. The breakthrough pressure at the cellulose membrane (pore size 8 μm) for the gas is higher than for the liquid.

The liquid is aspirated through the membrane and detector by two alternating 100 μL-syringe pumps (Cavro XL 3000, Tecan Systems, San Jose, CA, USA). The working principle of the bubble filter is based on the different breakthrough pressure of gas and liquid for narrow pores. A higher aspirating rate of the peristaltic pump than the syringe pumps as well as the membrane back pressure forced most of the gas to the peristaltic pump outlet. The syringe pumps aspirated with a flow rate of 10 μL/min.

3. Results and discussion

3.1. Knitted reactor applied at low flow rates

The performance of a knitted post-column reactor with regard to band broadening was tested in a model experiment as follows: the pesticide carbofuran was injected into a carrier liquid (10% methanol, 90% water) with a flow rate of 100 μL/min. The analyte was first detected by UV absorbance directly after the injection valve and then after it passed a Teflon tubing coil of 1 m length and an inner diameter of 0.5 mm. The tubing was first stretched linear and then it was knitted. The recorded chromatograms are shown in Fig. 3.

A comparison of the peak widths of the linear and the knitted tubing shows that the knitted reactor shows no significant improvement. According to the literature [28,32], the knitted reactor should have shown better performance. The peak broadening in the knitted reactor should be significant less than in the linear reactor due to an induced secondary flow. We assume that the application of knitted reactors is limited to higher flow rates in macroscopic tubing. Similar conclusions were drawn in [32].

3.2. Optimization of HPLC and SFEID

Prior the connection of a HPLC system to the enzyme inhibition assay, the loss of enzyme activity in the presence of organic

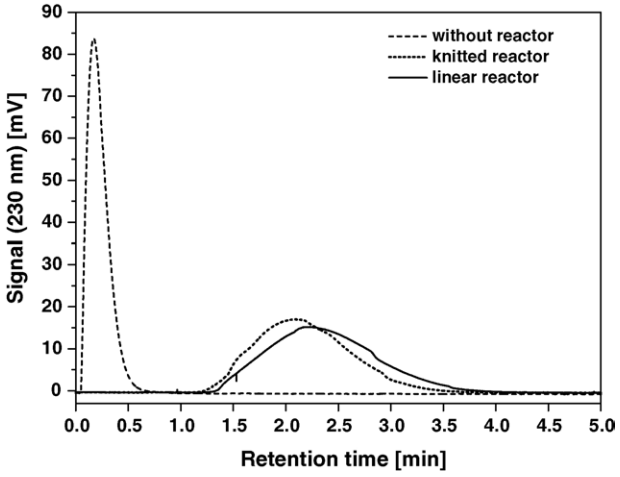

Fig. 3. Comparison of linear and knitted reactors. Injection of 20 μL of carbofuran in a carrier flow of aqueous methanol (10%) at a rate of 100 μL/min. The peak widths were compared between the signal resulting after connecting the detector and injection valve with a Teflon tubing (1 m length, 0.5 mm I.D., solid line), a knitted Teflon tubing (1 m length, 0.5 mm I.D., dotted line) and without reactor (direct connection to detector, dashed line). The dispersion was essentially the same for the linear and the knitted reactor.

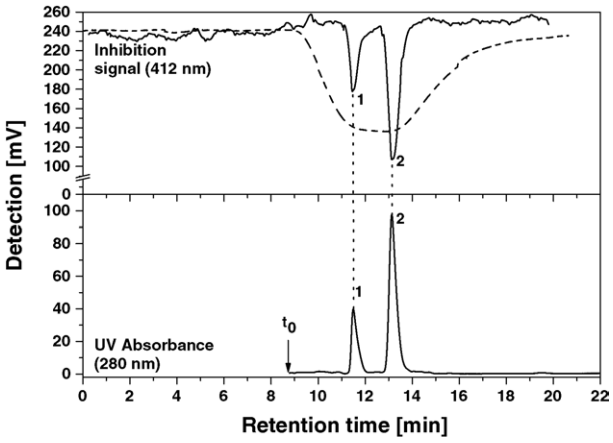

Fig. 5. Comparison of on-line HPLC–EID and HPLC–SFEID with HPLC–UV. Isocratic chromatography separated the pesticides carbofuran (1) and paraoxon-ethyl (2) as shown by the UV absorption signal (lower part of the chromatogram). The dashed line (- - -) in the upper part represents the inhibition signal recorded without segmentation (EID). The solid line (—) represents the inhibition signal with gas segmentation (SFEID). With the EID detector severe band-broadening occurs due to the parabolic flow profile and the long residence time in the reaction coil. Most of the resolution of HPLC is lost in the EID unit. Using the SFEID detector, the analytes are recorded with almost the same resolution as with the UV detection. Time offsets have been corrected for comparison.

solvents was examined. The effect of acetonitrile on AChE is significantly higher than the effect of methanol (Fig. 4). Therefore, methanol was chosen as organic solvent for the mobile phase. A methanol concentration up to ten percent did not lead to a significant loss of enzyme activity. In the subsequent experiments, one volume of methanolic sample solution was mixed with nine volumes of enzyme solution to avoid major influences of the mobile phase on the enzyme activity. Under these conditions, the baseline was sufficiently stable to identify the inhibition peaks.

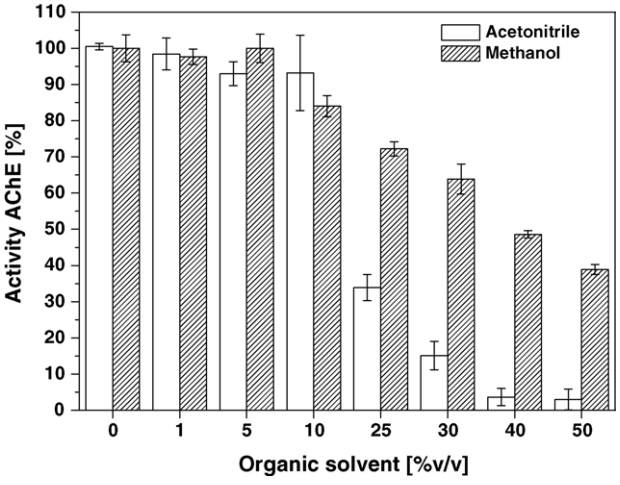

Fig. 4. The effects of acetonitrile and methanol on AChE in the microplate assay. The experiment was done in triplicates. Water/solvent mixtures (180 μL) were incubated with 20 μL of enzyme dilution for 5 min at 37 °C. After addition of 20 μL of substrate/reagent solution the remaining enzyme activity was determined as described in Section 2. The organic solvent concentration represents the amount of solvent in the well prior the substrate/reagent addition.

3.3. On-line analysis of inhibitors with HPLC–EID

With the optimized conditions obtained by the microplate assay, an EID without segmentation was directly coupled to a HPLC system. A mixture of a carbamate (carbofuran) and an organophosphate (paraoxon-ethyl) was injected as described in Section 2. The analytes were separated under isocratic conditions and recorded with the UV detector at 280 nm (Fig. 5, lower part). Due to the low flow rate and the small inner diameter of the capillary, the system is characterized by a low Reynolds number. Therefore, the flow scheme is strictly laminar and the flow profile is parabolic. The high resolution achieved by the chromatography was largely lost within the EID by longitudinal dispersion (Fig. 5, upper part, dotted line). The performance of the HPLC–EID is severely limited due to a very low peak capacity.

3.4. Reduction of band broadening by HPLC–SFEID

Here, we want to demonstrate the successful coupling of a HPLC system to an on-line enzyme inhibition detector with microliter segments. Air was used for the segmentation to avoid the extraction of analytes into the segmentation medium in the case of organic solvents. Quartz capillaries were preferred as reaction coils, because Teflon tubing is gas permeable, PEEK and stainless steel capillaries are opaque. Narrow capillaries lead to a tremendous reduction of reagent consumption in relation to larger tubing. The liquid in the segmented stream intermixes only within one segment apart from a thin liquid film on the tubing wall. To achieve a reproducible backmixing behavior, the air segments should be constant in size and spacing. According to Poiseuille's Law the pressure drop across the length of an open

tube is inversely proportional to the fourth power of the tubing radius. The injection of gas into long and narrow capillaries is relatively complicated to handle. The compressibility of inserted gas bubbles leads to unwanted pressure variations in the tube. The flow rate changes in the case of pressure-dependent pump characteristics. The equilibration of an air-segmented flow system with insertion of pressurized gas is tedious as also described in the literature [50]. To produce air segments reproducibly in a short equilibration time, the following steps should be pursued. First, all capillaries are filled with liquid. The T-piece for the air insertion is open and the pumps **1** and **2** (Fig. 1) deliver the liquid with a fixed flow rate. Now the peristaltic pump **3** is started. The speed of the pump is increased stepwise, until the pressure in the system is so low that air is aspirated through the third port of the T-piece. The system is essentially equilibrated when the air-liquid mixture reaches the peristaltic pump. The air segments are very uniform in size and are introduced in short intervals of ∼4.5 Hz (see Fig. 6 and movie in Supplementary materials).

The rotation rate and tubing size of the peristaltic pump determines the frequency of the air segments. The fluid segments had a volume of approximately 0.5 μL, whereas the bubbles had about half the volume. Bubble size and frequency were essentially independent of the solvent gradient. The addition of substrate/reagent solution to the segmented stream was achieved with a T-piece at a 40 times lower flow rate than the main stream to avoid a splitting of the bubbles. Since an electronic noise filtering was not possible with very short air intervals (Fig. 7, lower line), a bubble filter was engineered as described in Section 2.

Two syringe pumps in alternating action aspirated the liquid through a membrane. This setup worked very well under isocratic conditions (Fig. 7, upper line). A mixture of carbofuran and paraoxon-ethyl was injected under the same conditions as described above. After injection of a blank sample, no memory effect was observed (data not shown). The high resolution of the analytes achieved in the chromatography could be essentially preserved by the SFEID detector. The performance

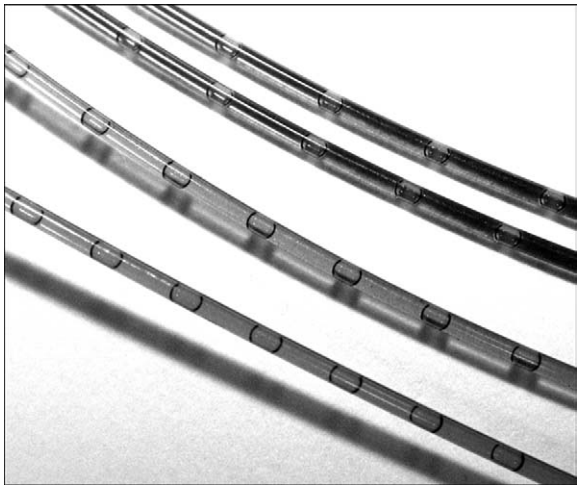

Fig. 6. Air segmentation in quartz capillaries of 660 μm outer diameter. See movie in Supplementary materials.

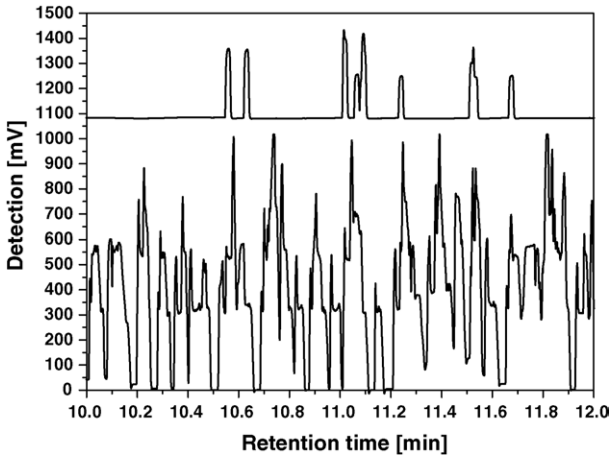

Fig. 7. A bubble filter leads to improved signal quality. The air segments were inserted into the capillary at a frequency of ∼4.5 Hz. The signal recorded without the bubble filter is shown in the lower line. The upper line (offset 700 mV) shows the signal recorded with the bubble filter. The membrane removed the inserted bubbles with an efficiency of about 98%.

of the HPLC–SFEID in comparison with the non-segmented HPLC–EID is shown in Fig. 5. With the gas-segmented flow in the enzyme inhibition unit, the band broadening was reduced significantly.

3.5. LOD and peak width with HPLC–SFEID

By injection of different concentrations of carbofuran and paraoxon mixtures into the HPLC–SFEID system, a calibration curve was obtained (Fig. 8). Carbofuran could be detected down to 13 ng and paraoxon down to 7 ng (S/N > 3, injected mass). For comparison, a microplate assay was carried out with the same incubation time and theoretical sample dilution factors as in the

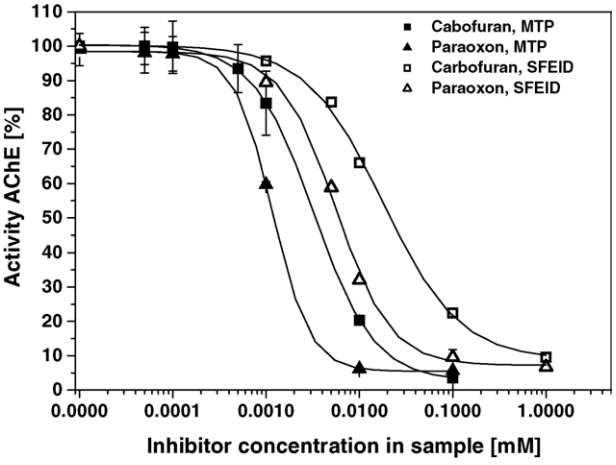

Fig. 8. Calibration curves of paraoxon-ethyl and carbofuran were recorded with the HPLC–SFEID (open symbols) and the microtiter plate (solid symbols) as comparison. The incubation time was equal for each experiment. The IC_{50}-value for carbofuran was 3.2 μM for the MTP assay and 17.8 μM with the HPLC–SFEID. The IC_{50}-value for paraoxon was 1.2 μM for the MTP assay and 5.6 μM with the HPLC–SFEID. The higher IC_{50}-values for the HPLC–SFEID result mainly from analyte dilution in the isocratic chromatography, the makeup-flow splitter and the reaction coil.

Table 1
LOD and IC_{50} values for carbofuran and paraoxon-ethyl with MTP and HPLC–SFEID

		Carbofuran			Paraoxon-ethyl		
		ng	μM	mg/L	ng	μM	mg/L
LOD	SFEID	13	3.0	0.66	7.4	1.3	0.36
	MTP	4.9	1.1	0.24	3.2	0.58	0.16
IC_{50}	SFEID[a]	79	18	3.9	31	5.6	1.5
	MTP[b]	14	32	0.72	6.4	1.2	0.32

[a] The error of the IC_{50} values determined from the calibration curve (Fig. 8) is 14% for Carbofuran and 9.7% for Paraoxon.
[b] The error of the IC_{50} values determined from the calibration curve (Fig. 8) is 1.9% for Carbofuran and 2.6% for Paraoxon.

HPLC–SFEID. The LOD defined as a twenty percent decrease of enzyme activity was 5 ng for carbofuran and 3 ng for paraoxon in the microplate assay (see Table 1).

The IC_{50}-values of the HPLC–SFEID calculated from the injected mass were higher by a factor of about five compared to the MTP assay. Intra-column dispersion contributed with a factor of two to the loss of sensitivity considering the effective analyte concentration at the peak maximum in the UV-detector. Therefore, extra-column dispersion caused by fluidic components decreases the sensitivity by a factor of about 2–3.

The maximum residue limits for pesticides in drinking water set by the EU are 0.1 and 0.5 μg/L (sum), respectively. These limits are not toxicity-motivated and based on the precautionary principle. With the integration of an enrichment step prior to the chromatographic separation the LOD should be sufficient to detect toxic compounds at or below the above mentioned limits.

The performance of the HPLC–SFEID was demonstrated in the following example. A model mixture of two carbamates (pirimicarb, carbaryl), two organophosphates (paraoxon-ethyl, dichlorvos) and one organothiophosphate (chlorpyrifos-methyl) was injected into the system at a concentration of 100 μM

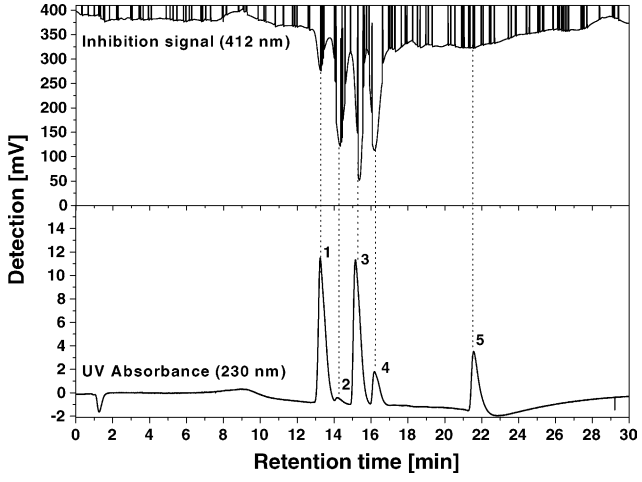

Fig. 9. HPLC–SFEID with a mixture of the pesticides pirimicarb (1); dichlorvos (2); carbaryl (3); paraoxon-ethyl (4) and chlorpyrifos-methyl (5). The inhibition signal was satisfactory, although the separation of liquid and gas was not complete. Residual bubbles flowing through the detector cause positive recorder signals. The inhibitor signal of the organothiophosphate chlorpyrifos-methyl (5) was detected after oxidation with NBS (data shown in Table 2).

Table 2
Retention time t_{Ret} and peak width $w_{1/2}$ of the HPLC–SFEID separation of five pesticides in (min)

Pesticide	UV (230 nm)		SFEID (412 nm)		
	t_{Ret}	$w_{1/2}$[a]	t_{Ret}	t_{Ret} (with 7.7 min offset)	$w_{1/2}$[b]
Pirimicarb	13.25	0.39	20.85	13.17	0.44
Dichlorvos	14.18	0.34	21.92	14.24	0.49
Carbaryl	15.16	0.40	22.96	15.28	0.43
Paraoxon-ethyl	16.19	0.40	23.78	16.10	0.57
Chlorpyrifos-methyl	21.56	0.41	–	–	–
Chlorpyrifos-methyl (after oxidation with NBS)	17.61	0.51	25.26	17.58	0.59

[a] The full width at half maximum was determined with an error of 5% for the UV detector signal.
[b] The full width at half maximum was determined with an error of 15% for the SFEID signal.

for each pesticide. The separation was performed by a methanol/water/acetic acid gradient on a reversed phase column as described in Section 2. Unfortunately, the bubble filter worked less efficient under these conditions. Varying viscosity and surface tension due to the gradient elution caused the occasional breakthrough of bubbles due to the changing back pressure of the liquid and gas at the filter paper. Nevertheless, useful inhibition curves could be recorded (Fig. 9).

All five pesticides could be separated and subsequently detected by UV and four of the pesticides with the SFEID-detector, too. The fifth pesticide chlorpyrifos-methyl showed no signal with the SFEID-detector, because thiophosphates do not inhibit AChE significantly. Dichlorvos (2) has no conjugated double bonds. Hence it shows a very weak absorbance, even at 230 nm. A sensitive analysis of dichlorvos usually has to be performed by GC or LC/MS. With the HPLC–SFEID dichlorvos was easily detected by the strong inhibitory effect on AChE (see peak 2 in Fig. 9).

For the separation of complex mixtures, a chromatogram should resolve as many peaks as possible. For the peak width at half height $w_{1/2}$ the value of paraoxon-ethyl as a representative value was chosen. In the experiment, the peak width of the UV-detector signal (0.40 ± 0.02 min) was ~30% less than the peak width of the SFEID signal (0.57 ± 0.09 min).

The loss in resolution as well as the higher detection limit of the HPLC–SFEID compared to the microtiter plate assay (Table 1) is partly due to the residual dispersion in the segmented flow. Depending on the properties of the tubing material and the liquid, the surface of the tube wall is usually wetted. Liquid from one segment is therefore deposited on the tube wall in the form of a liquid film and is picked up by the subsequent segment. This substance transfer from one segment to another leads to some longitudinal dispersion.

4. Conclusions

This work demonstrates that chromatography with gas-segmented biochemical detectors is a powerful tool for effect-directed analysis. To limit reagent consumption, the system

works in the flow range of 100 μL/min. In these micro-scale systems, band broadening due to longitudinal dispersion is one of the main problems. The use of gas-segmentation is particularly advantageous for the analysis of complex mixtures, because the high resolution of modern liquid chromatography is essentially retained in the reaction coils of the homogenous enzyme inhibition detection. This was demonstrated by separation of insecticide mixtures with isocratic and gradient chromatography, respectively, followed by the online detection of acetylcholinesterase inhibition.

Acknowledgements

The research was supported by the German Federal Ministry of Education and Research (BMBF 02WU0331) and the Max Buchner Research Foundation. We thank our project partners Dr. Bachmann and Dr. Schulz at the Institute of Technology Biochemistry (University of Stuttgart) and Prof. Bilitewski and Ms. Lüderitz at the German Research Center for Biotechnology (Braunschweig) for their valuable cooperation. We also like to thank Dr. Kowalczyk and Dr. Hartmann from the Chair of Fluid Mechanic and Process Automation (Technische Universität München, Freising) for fruitful discussions and Mr. Dollinger and Mr. Wiesemann from our technical workshop.

Appendix A. Supplementary data

Supplementary data associated with this article can be found, in the online version, at doi:10.1016/j.chroma.2005.08.081.

References

[1] N. van der Hoeven, Acta Biotheor. 52 (2004) 201.
[2] M. Farré, D. Barceló, Trends Anal. Chem. 22 (2003) 299.
[3] W. Brack, Anal. Bioanal. Chem. 377 (2003) 397.
[4] U. Bilitewski, G. Brenner-Weiss, P.D. Hansen, B. Hock, E. Meulenberg, G. Müller, U. Obst, H. Sauerwein, F.W. Scheller, R. Schmid, G. Schnabl, F. Spener, Trends Anal. Chem. 19 (2000) 428.
[5] R.I.L. Eggen, H. Segner, Anal. Bioanal. Chem. 377 (2003) 386.
[6] G. Brenner-Weiss, U. Obst, Anal. Bioanal. Chem. 377 (2003) 408.
[7] M.G. Weller, Fresenius' J. Anal. Chem. 366 (2000) 635.
[8] M. Seifert, G. Brenner-Weiss, S. Haindl, M. Nusser, U. Obst, B. Hock, Fresenius' J. Anal. Chem. 363 (1999) 767.
[9] M.D.L. de Castro, M.C. Herrera, Biosens. Bioelectron. 18 (2003) 279.
[10] M.W.F. Nielen, E.O. van Bennekom, H.H. Heskamp, J.A. van Rhijn, T.F.A. Bovee, L.A.P. Hoogenboom, Anal. Chem. 76 (2004) 6600.
[11] A. Zeck, M.G. Weller, R. Niessner, Anal. Chem. 73 (2001) 5509.
[12] C. Weins, H. Jork, J. Chromatogr. A 750 (1996) 403.
[13] D.A. van Elswijk, T. Schenk, U.R. Tjaden, J. van der Greef, H. Irth, in: B. Hock (Ed.), Bioresponse-Linked Instrumental Analysis, Teubner, Stuttgart, Germany, 2001, p. 9.
[14] D.A. van Elswijk, U.P. Schobel, E.P. Lansky, H. Irth, J. van der Greef, Phytochemistry 65 (2004) 233.
[15] A.J. Oosterkamp, R. van der Hoeven, W. Glassgen, B. König, U.R. Tjaden, J. van der Greef, H. Irth, J. Chromatogr. B 715 (1998) 331.
[16] E.S. Lutz, H. Irth, U.R. Tjaden, J. van der Greef, J. Chromatogr. A 755 (1996) 179.
[17] J. Emnéus, G. Marko-Varga, J. Chromatogr. A 703 (1995) 191.
[18] M. Bartolini, V. Cavrini, V. Andrisano, J. Chromatogr. A 1031 (2004) 27.
[19] T. Schenk, N. Appels, D.A. van Elswijk, H. Irth, U.R. Tjaden, J. van der Greef, Anal. Biochem. 316 (2003) 118.
[20] T. Schenk, J. Breel, P. Koevoets, S. van den Berg, A.C. Hogenboom, H. Irth, U.R. Tjaden, J. van der Greef, J. Biomol. Screen. 8 (2003) 421.
[21] D.A. van Elswijk, O. Diefenbach, S. van der Berg, H. Irth, U.R. Tjaden, J. van der Greef, J. Chromatogr. A 1020 (2003) 45.
[22] K. Ingkaninan, C.M. de Best, R. van der Heijden, A.J.P. Hofte, B. Karabatak, H. Irth, U.R. Tjaden, J. van der Greef, R. Verpoorte, J. Chromatogr. A 872 (2000) 61.
[23] I.K. Rhee, N. Appels, B. Hofte, B. Karabatak, C. Erkelens, L.M. Stark, L.A. Flippin, R. Verpoorte, Biol. Pharm. Bull. 27 (2004) 1804.
[24] A.R. de Boer, T. Letzel, D.A. van Elswijk, H. Lingeman, W.M.A. Niessen, H. Irth, Anal. Chem. 76 (2004) 3155.
[25] H.A. Stone, S. Kim, AIChE J. 47 (2001) 1250.
[26] U.A.Th. Brinkman, R.W. Frei, H. Lingeman, J. Chromatogr. 492 (1989) 251.
[27] R.W. Frei, A.H.M.T. Scholten, J. Chromatogr. Sci. 17 (1979) 152.
[28] R.S. Deelder, A.T.J.M. Kuijpers, J.H.M. Vandenberg, J. Chromatogr. 255 (1983) 545.
[29] H. Engelhardt, B. Lillig, J. High Resol. Chromatogr. Chromatogr. Commun. 8 (1985) 531.
[30] H. Engelhardt, U.D. Neue, Chromatographia 15 (1982) 403.
[31] O. Kuhlmann, G.J. Krauss, J. Pharm. Biomed. Anal. 16 (1997) 553.
[32] A.D. Kaufman, P.T. Kissinger, Curr. Sep. 17 (1998) 9.
[33] L.R. Snyder, J. Chromatogr. 125 (1976) 287.
[34] W. Salman, P. Angeli, A. Gavriilidis, Chem. Eng. Technol. 28 (2005) 509.
[35] L.T. Skeggs, Am. J. Clin. Pathol. 28 (1957) 311.
[36] L.T. Skeggs, Clin. Chem. 46 (2000) 1425.
[37] J.R. Lang, I.L. Honigberg, J.T. Stewart, J. Chromatogr. 252 (1982) 288.
[38] J.C. Gfeller, G. Frey, R.W. Frei, J. Chromatogr. 142 (1977) 271.
[39] K.A. Ramsteiner, W.D. Hörmann, J. Chromatogr. 104 (1975) 438.
[40] K.B. Sipponen, J. Chromatogr. 389 (1987) 87.
[41] H.A. Moye, T.E. Wade, Anal. Lett. 9 (1976) 891.
[42] A. Grodian, J. Metze, T. Henkel, K. Martin, M. Roth, J.M. Köhler, Biosens. Bioelectron. 19 (2004) 1421.
[43] J.M. Köhler, T. Henkel, A. Grodrian, T. Kirner, M. Roth, K. Martin, J. Metze, Chem. Eng. J. 101 (2004) 201.
[44] J.M. Köhler, T. Kirner, Sens. Actuators A 119 (2005) 19.
[45] V. Linder, S.K. Sia, G.M. Whitesides, Anal. Chem. 77 (2005) 64.
[46] J.W. Bartsch, H.D. Tran, A. Waller, A.A. Mammoli, T. Buranda, L.A. Sklar, B.S. Edwards, Anal. Chem. 76 (2004) 3810.
[47] H. Song, J.D. Tice, R.F. Ismagilov, Angew. Chem. Int. Ed. 42 (2003) 768.
[48] G.N. Doku, W. Verboom, D.N. Reinhoudt, A. van den Berg, Tetrahedron 61 (2005) 2733.
[49] J.H. Tsai, L.W. Lin, Sens. Actuators A 97 (2002) 665.
[50] J.L. Edwards, R. Bauman, D.M. Spence, Anal. Chim. Acta 401 (1999) 209.
[51] H. Schulze, S. Vorlova, F. Villatte, T.T. Bachmann, R.D. Schmid, Biosens. Bioelectron. 18 (2003) 201.
[52] G.L. Ellman, K.D. Courtney, V. Andres, R.M. Featherstone, Biochem. Pharmacol. 7 (1961) 88.